iScience

CellPress
OPEN ACCESS

Article

Reduced acetylation of TFAM promotes bioenergetic dysfunction in the failing heart

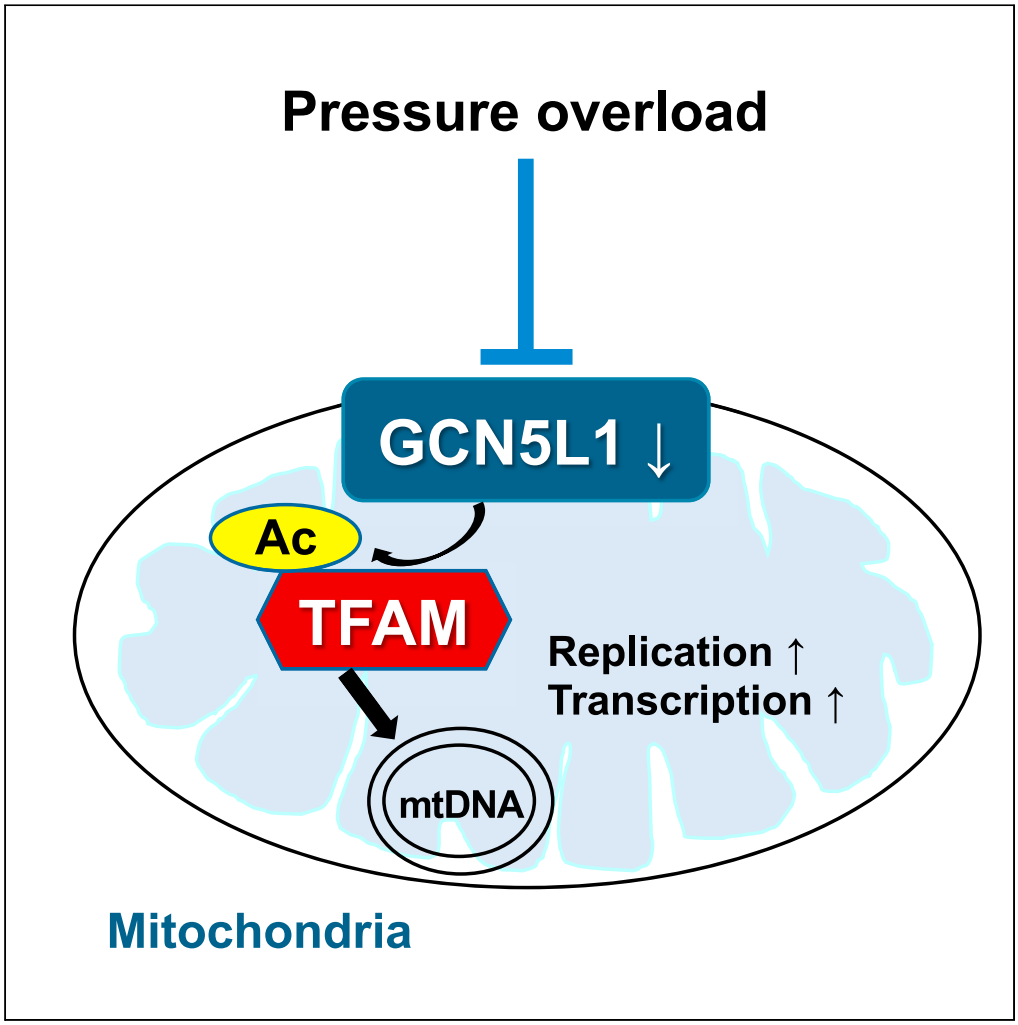

Manling Zhang, Ning Feng, Zishan Peng, ..., Brett A. Kaufman, Michael N. Sack, Iain Scott

zhangm5@upmc.edu (M.Z.)
iain.scott@pitt.edu (I.S.)

Highlights

Reduced GCN5L1 expression in the failing heart promotes contractile dysfunction

Mitochondrial DNA levels are reduced in stressed cardiac-specific GCN5L1 knockout mice

GCN5L1 modulation regulates bioenergetics in myocytes

GCN5L1-mediated acetylation of TFAM promotes increased mitochondrial DNA levels

Zhang et al., iScience *26*, 106942
June 16, 2023 © 2023 The Author(s).
https://doi.org/10.1016/j.isci.2023.106942

iScience

CellPress
OPEN ACCESS

Article

Reduced acetylation of TFAM promotes bioenergetic dysfunction in the failing heart

Manling Zhang,[1,2,3,10,11,*] Ning Feng,[1,2,3,10] Zishan Peng,[1,2] Dharendra Thapa,[4] Michael W. Stoner,[1,2,5] Janet R. Manning,[1,2,5] Charles F. McTiernan,[1,2] Xue Yang,[1,2] Michael J. Jurczak,[5,6] Danielle Guimaraes,[1,2,7,9] Krithika Rao,[1,2,7] Sruti Shiva,[1,2,7] Brett A. Kaufman,[1,2,5] Michael N. Sack,[8] and Iain Scott[1,2,5,11,12,*]

SUMMARY

General control of amino acid synthesis 5-like 1 (GCN5L1) was previously identified as a key regulator of protein lysine acetylation in mitochondria. Subsequent studies demonstrated that GCN5L1 regulates the acetylation status and activity of mitochondrial fuel substrate metabolism enzymes. However, the role of GCN5L1 in response to chronic hemodynamic stress is largely unknown. Here, we show that cardiomyocyte-specific GCN5L1 knockout mice (cGCN5L1 KO) display exacerbated heart failure progression following transaortic constriction (TAC). Mitochondrial DNA and protein levels were decreased in cGCN5L1 KO hearts after TAC, and isolated neonatal cardiomyocytes with reduced GCN5L1 expression had lower bioenergetic output in response to hypertrophic stress. Loss of GCN5L1 expression led to a decrease in the acetylation status of mitochondrial transcription factor A (TFAM) after TAC *in vivo*, which was linked to a reduction in mtDNA levels *in vitro*. Together, these data suggest that GCN5L1 may protect from hemodynamic stress by maintaining mitochondrial bioenergetic output.

INTRODUCTION

Heart failure remains one of the leading causes of death and hospital admission in the US.[1] Despite improved therapeutic approaches, the prognosis of heart failure remains poor, with ~50% mortality in 5 years.[2,3] As such, there is considerable enthusiasm for further exploration of the pathogenic mechanisms underlying heart failure, and the development of novel mechanism-based therapeutic strategies. Metabolic derangements and poor cardiac energy production are hallmarks of heart failure,[4–6] and systems that regulate cardiac bioenergetics represent a potential target for therapeutic intervention.

Mitochondrial bioenergetic output is controlled by several key mechanisms related to fuel import, substrate oxidation, and electron transport complex function. Mitochondrial transcription factor A (TFAM) controls the replication, copy number, and stability of mitochondrial DNA (mtDNA), and is necessary for the maintenance of the mitochondrial electron transport chain.[7,8] The abundance of mtDNA is decreased in heart failure, and overexpression of TFAM improves cardiac function after myocardial infarction.[9] To date, the molecular mechanisms governing the regulation of TFAM in response to pathological stresses in the heart remain poorly understood.

General control of amino acid synthesis 5-like 1 (GCN5L1) was previously identified as a mitochondrial acetyltransferase-related protein.[10] GCN5L1-mediated acetylation is implicated in the regulation of fatty acid oxidation, glucose oxidation, and mitochondrial respiration under various conditions.[11–13] However, whether GCN5L1 plays a role in the regulation of cardiac bioenergetics in response to hemodynamic stress is unknown. Using novel cardiac-specific GCN5L1 KO mice (cGCN5L1 KO), we show that GCN5L1 is required to protect hearts from pressure overload-induced heart failure. Mechanistic studies reveal that GCN5L1 enhances cardiac energetics in response to pressure overload (transaortic constriction; TAC) by maintaining mtDNA abundance via lysine acetylation of TFAM. These data suggest that approaches which support GCN5L1 expression and/or TFAM acetylation may offer therapeutic benefits in future translational studies on heart failure.

[1]Vascular Medicine Institute, Department of Medicine, University of Pittsburgh, Pittsburgh, PA 15261, USA

[2]Division of Cardiology, Department of Medicine, University of Pittsburgh, Pittsburgh, PA 15261, USA

[3]Pittsburgh Veteran Affairs Medical Center, Pittsburgh, PA 15240, USA

[4]Division of Exercise Physiology, West Virginia University School of Medicine, Morgantown, WV 26506, USA

[5]Center for Metabolism and Mitochondrial Medicine, Department of Medicine, University of Pittsburgh, Pittsburgh, PA 15261, USA

[6]Division of Endocrinology and Metabolism, Department of Medicine, University of Pittsburgh, Pittsburgh, PA 15261, USA

[7]Department of Pharmacology and Chemical Biology, University of Pittsburgh, Pittsburgh, PA 15261, USA

[8]Intramural Research Program, National Heart, Lung, and Blood Institute, Bethesda, MD 20892, USA

[9]Present address: Department of Pharmacology, Ribeirao Preto Medical School, University of Sao Paulo, Sao Paulo, Brazil

[10]These authors contributed equally

[11]Senior author

[12]Lead contact

*Correspondence: zhangm5@upmc.edu (M.Z.), iain.scott@pitt.edu (I.S.)

https://doi.org/10.1016/j.isci.2023.106942

This is an open access article under the CC BY-NC-ND license (http://creativecommons.org/licenses/by-nc-nd/4.0/).

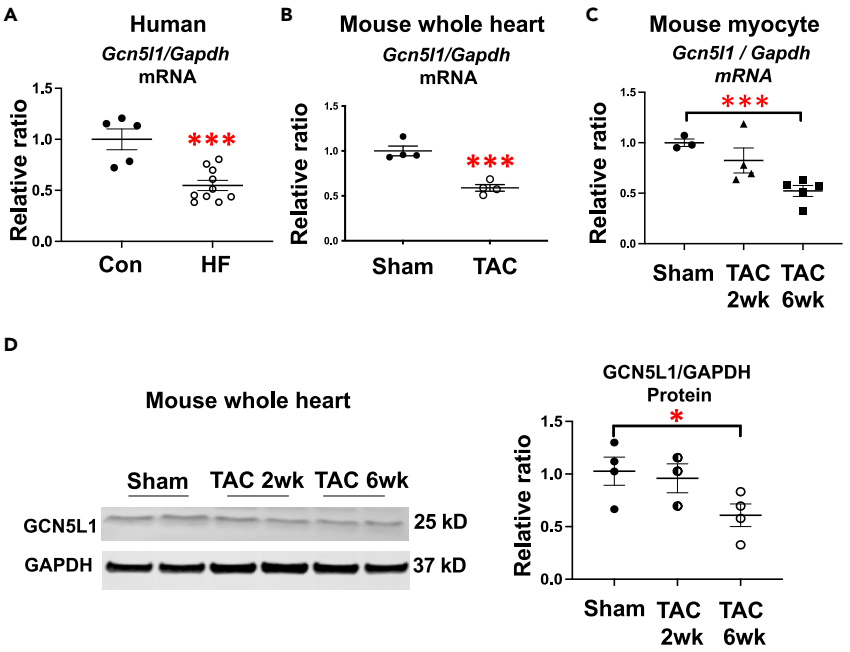

Figure 1. Myocardial GCN5L1 level is decreased in dilated cardiomyopathy

(A–D) GCN5L1 mRNA level was significantly decreased in patients with non-ischemic cardiomyopathy (n = 5–10) and mouse failing hearts after TAC (n = 4). GCN5L1 mRNA (C) and protein level (D) was significantly decreased in isolated myocytes and whole tissue from decompensated failing hearts (6 weeks after TAC), but there was no significant change GCN5L1 expression at the earlier cardiac hypertrophy stage (2 weeks after TAC; n = 3–4). Data are shown as means ± SEM. *p < 0.05, ***p < 0.001 vs. sham group.

RESULTS

Myocardial GCN5L1 level is decreased in dilated cardiomyopathy

To investigate the role of GCN5L1 in heart failure, we first examined the expression of GCN5L1 in human and mouse failing hearts. We found that GCN5L1 mRNA expression was significantly reduced in explanted hearts from patients with non-ischemic cardiomyopathy (Figure 1A), and in mouse hearts subjected to TAC (Figure 1B). We next examined GCN5L1 expression levels in different stages of heart failure development. We found there was no significant change in GCN5L1 mRNA expression or protein abundance in the early cardiac hypertrophy stage (2 weeks after TAC) in either isolated adult mouse cardiomyocytes or whole heart tissue (Figures 1C and 1D). However, GCN5L1 levels were significantly decreased in the dilated, decompensated heart failure stage (6 weeks after TAC) in both cases (Figures 1C and 1D). These findings suggest that decreased myocardial GCN5L1 levels may play a role in heart failure progression.

Given that GCN5L1 is a mitochondrial acetyltransferase protein, we next inspected total mitochondrial acetylation levels in TAC hearts to determine whether its reduced level affected global mitochondrial lysine acetylation status. However, we found that there was no change in total mitochondrial protein acetylation throughout the different heart failure stages (Figure S1A). This suggested that either other acetylation/deacetylation processes are modulated to compensate for the gradual loss of GCN5L1-mediated acetylation after TAC, or that loss of GCN5L1 expression in response to pressure overload leads to targeted reductions in the acetylation levels of specific mitochondrial proteins.

To test whether changes in other acetylation regulators were responsible for the lack of global mitochondrial acetylation changes observed during heart failure development, we examined the expression of the key mitochondrial deacetylase, Sirt3, in TAC hearts. There was no significant change in Sirt3 mRNA level throughout the different heart failure stages (Figure S1B), suggesting Sirt3 is unlikely to be responsible for any compensation in response to decreased GCN5L1 levels. From these data, we conclude that heart failure progression leads to a decrease in GCN5L1 expression, and that this change is likely to have a

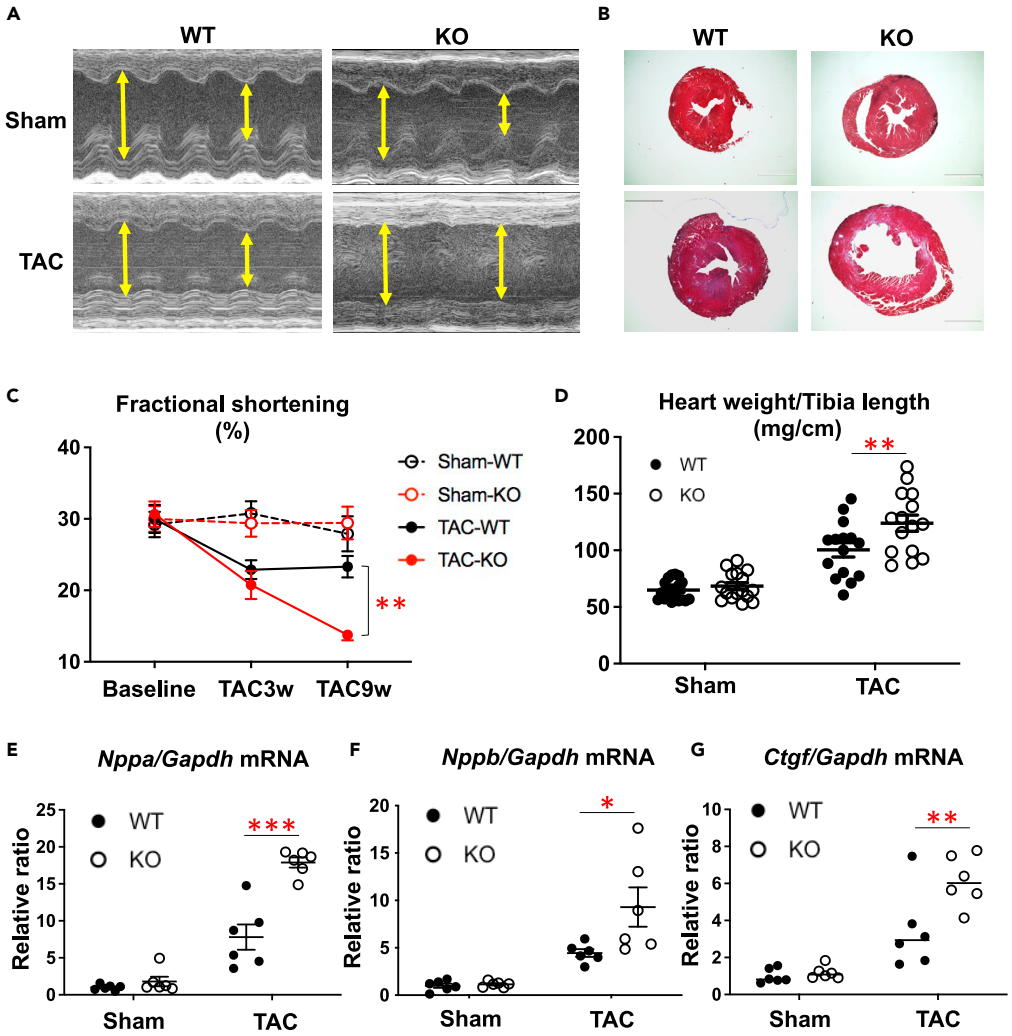

Figure 2. Cardiac-specific GCN5L1 KO mice display exacerbated heart failure in response to pressure overload

(A–B) Representative echocardiography and histology of WT and cGCN5L1 KO mice subjected to sham or TAC. Scale bar = 1 mm.

(C) Compared to WT controls, cGCN5L1 KO mice showed further decreased fractional shortening after TAC (n = 15).

(D) cGCN5L1 KO mouse heart weight was increased relative to WT controls after TAC (n = 15).

(E–G) ANP (*Nppa*), BNP (*Nppb*), and CTGF (*Ctgf*) mRNA were increased in cGCN5L1 KO mice after TAC (n = 6). Data are shown as means ± SEM. *p < 0.05, **p < 0.01, ***p < 0.001 vs. TAC-WT group.

regulatory effect on specific mitochondrial target proteins, as opposed to a significant effect on global mitochondrial acetylation levels.

Cardiomyocyte-specific GCN5L1 KO mice display exacerbated heart failure after TAC

To determine the importance of decreased GCN5L1 levels in heart failure development, cardiac-specific GCN5LI knockout (cGCN5L1 KO) mice were generated by crossing floxed GCN5L1 mice with constitutive α-myosin heavy chain-Cre mice (Figure S2). Cardiac function in cGCN5L1 KO mice was similar to wild-type (WT) mice to at least one year of age under non-stressed conditions (Figure S2). To understand the role of GCN5L1 during cardiac stress, WT littermate controls and cGCN5L1 KO mice aged 10–12 weeks were subjected to TAC. Compared to WT littermate controls, cGCN5L1 KO mice developed accelerated heart failure progression after TAC, with increased dilation of left ventricular chamber (Figures 2A and 2B), decreased fractional shortening (Figure 2C), increased heart weight (Figure 2D), and augmented fetal gene (Figures 2E and 2F) or fibrosis marker (Figure 2G) expression. Male and female mouse data were

combined based on the observation that male and female cGCN5L1 KO mice showed similar outcomes after TAC compared to WT controls (Figure S3). Overall, these studies suggest that cardiac GCN5L1 expression is required to protect the heart against pathological stress.

Ablation of GCN5L1 expression in cardiomyocytes reduces ETC protein abundance, complexes activity, and mtDNA levels

We next examined the mechanism underlying decreased cardiac function in cGCN5L1 KO mice in response to pressure overload. Strikingly, the abundance of mitochondrial electron transport chain (ETC) proteins from Complex I, III, IV, and the ATP synthase was significantly reduced in cGCN5L1 KO mice after TAC relative to WT controls (Figure 3A). In contrast, there was no difference in protein abundance from Complex II (Figure 3A), which unlike the other complexes contains no mtDNA gene products. We therefore examined mtDNA levels in mice after sham or TAC surgery, and found that cGCN5L1 KO mice displayed a significant decrease in mt-ND2 (complex I) and mt-ATP6 (ATP synthase) expression after TAC relative to their WT controls (Figure 3B). To determine whether the observed decrease in ETC protein levels was due to general reductions in mitochondrial protein expression in whole heart tissue relative to total cellular protein, or are specifically a result of decreased ETC protein abundance relative to other mitochondrial proteins, we measured ETC protein expression in isolated mitochondria from WT control and cGCN5L1 KO mice subject to TAC. In common with whole heart tissue, ETC proteins from Complex I, III, IV, and the ATP synthase were significantly decreased in isolated mitochondria from cGCN5L1 KO mice hearts (Figure 3C). This suggests that ETC proteins are specifically downregulated in cGCN5L1 KO mice subject to TAC, relative to total mitochondrial protein. Finally, we measured Complex I and IV activity in the extracted mitochondria. Consistent with the observed decrease in ETC protein levels, Complex I and IV activity was significantly decreased in mitochondria isolated from cGCN5L1 KO mice hearts after TAC relative to WT controls under the same conditions (Figure 3D).

GCN5L1 knockdown impairs mitochondrial function in hypertrophic cardiomyocytes

As the decrease in ETC protein and mtDNA levels suggested a negative impact on mitochondrial bioenergetics, we modeled how decreased GCN5L1 levels would affect bioenergetic output in neonatal rat cardiomyocytes (NRCMs). In NRCMs stimulated with the hypertrophy inducer phenylephrine, GCN5L1 siRNA knockdown resulted in greater cell surface area (Figure S4A) and fetal gene reprogramming (Figure S4B,C), matching the phenotype observed *in vivo* after TAC. Using Seahorse XF respirometry in control and hypertrophied NRCMs, we found that basal oxygen consumption rate (OCR), maximal OCR, and ATP synthesis-linked OCR were significantly decreased with GCN5L1 knockdown in the presence of phenylephrine (Figures 4B–4E). Taken together, these findings suggest that GCN5L1 abundance governs mitochondrial bioenergetic output in cardiomyocytes during hemodynamic stress, and that reduced GCN5L1 levels promote energy deficits at the onset of hypertrophy.

Adenoviral-mediated GCN5L1 overexpression restores bioenergetic output in hypertrophic cardiomyocytes

As loss of GCN5L1 expression negatively impacted mitochondrial bioenergetics in stressed hearts, we hypothesized that increasing GCN5L1 abundance may protect cardiomyocytes from hypertrophic remodeling. Indeed, adenoviral-mediated GCN5L1 overexpression (Figure 5A) inhibited fetal gene reprogramming in NRCMs treated with phenylephrine (Figures 5B and 5C), suggesting that increased GCN5L1 levels may be cardioprotective. We then examined whether GCN5L1 overexpression would reverse the bioenergetic decline observed in GCN5L1-depleted cells, and found that phenylephrine-treated NRCMs transduced with adenoviral GCN5L1 increased maximal OCR and ATP synthesis-linked OCR (Figures 5D–5G). Combined, these data suggest that increased GCN5L1 abundance inhibits the progression of hypertrophic remodeling and limits bioenergetic dysfunction in stressed cardiomyocytes.

GCN5L1-mediated TFAM acetylation promotes increased mtDNA levels in cardiomyocytes

We next investigated potential mechanisms underlying GCN5L1 control of mitochondrial bioenergetics in failing hearts. Consistent with previous reports,[12] we found that total mitochondrial protein acetylation levels were significantly decreased in cGCN5L1 KO mice relative to WT controls (Figure S5), supporting the concept that GCN5L1 is an important component of the mitochondrial acetylation regulatory machinery *in vivo*. As our initial studies suggested that a reduction in mtDNA levels may underpin respiratory

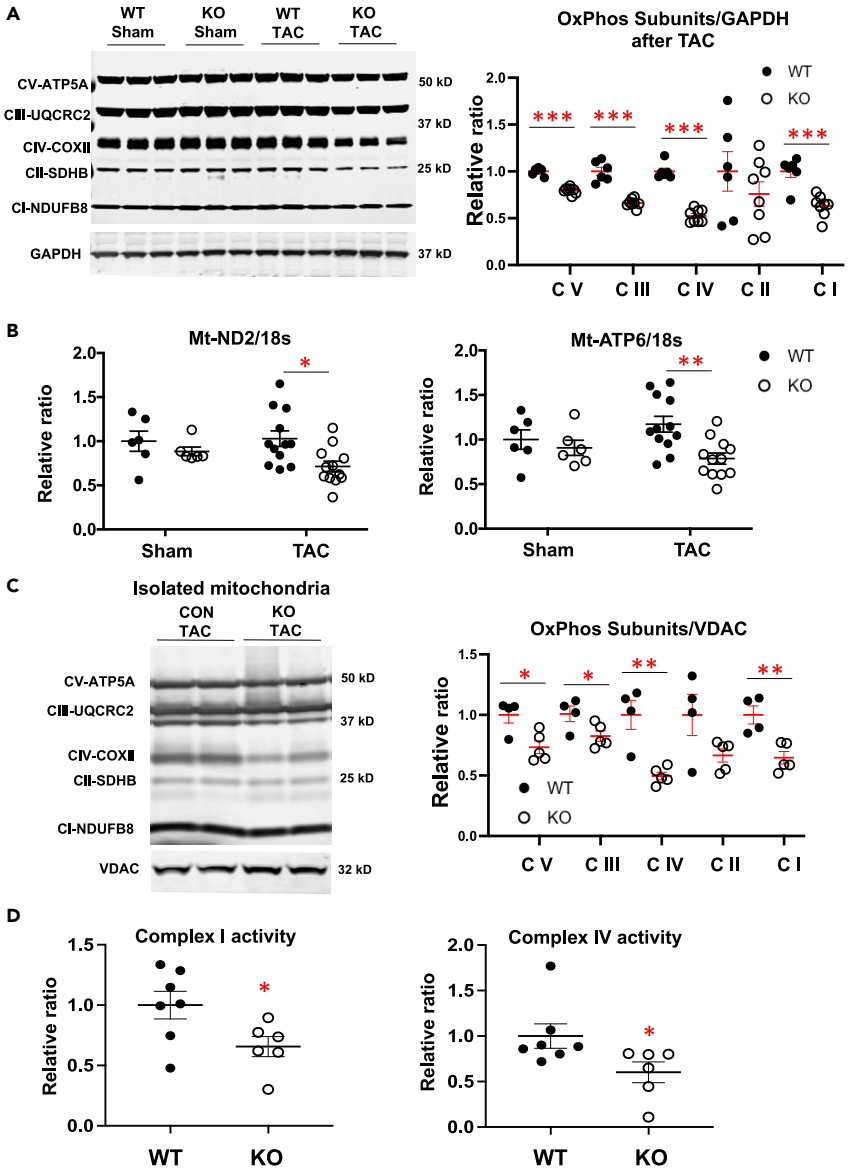

Figure 3. Mitochondrial ETC proteins, complexes activity, and mitoDNA copy number are decreased in cGCN5L1 KO mice subjected to TAC

(A) OXPHOS cocktail western blot showed that mitochondrial proteins including NDUFB8 (complex I), UQCRC2 (complex III), COXII (complex IV), and ATP5A (ATP synthase) were decreased in TAC cGCN5L1 KO mice, compared to WT controls (n = 6 in WT, n = 8 in KO). There was no significant difference in SDHB (Complex II).

(B) Mitochondrial DNA copy number, assessed by mt-ND2/18s RNA and mt-ATP6/18s RNA, was reduced in cGCN5L1 KO mice subjected to TAC (n = 6 in sham groups, n = 12 in TAC groups).

(C) In isolated mitochondria from TAC WT and cGCN5L1 KO mice hearts, NDUFB8 (complex I), UQCRC2 (complex III), COXII (complex IV), and ATP5A (ATP synthase) were decreased in cGCN5L1 KO mice (n = 4–5).

(D) Complex I and IV activity were decreased in mitochondria isolated from cGCN5L1 KO mice hearts (n = 6–7). Data are shown as means ± SEM. *p < 0.05, **p < 0.01, ***p < 0.001.

deficits in cGCN5L1 KO mice, we examined whether the acetylation status of key regulators of mitochondrial gene expression was altered following cardiomyocyte-specific GCN5L1 depletion. We found that TFAM acetylation levels were decreased in cGCN5L1 KO mice hearts subjected to TAC relative to WT controls, which occurred in the absence of changes to TFAM protein levels (Figures 6A–6C). To determine if GCN5L1 directly regulated TFAM acetylation levels *in vitro*, we transduced NRCMs with control or

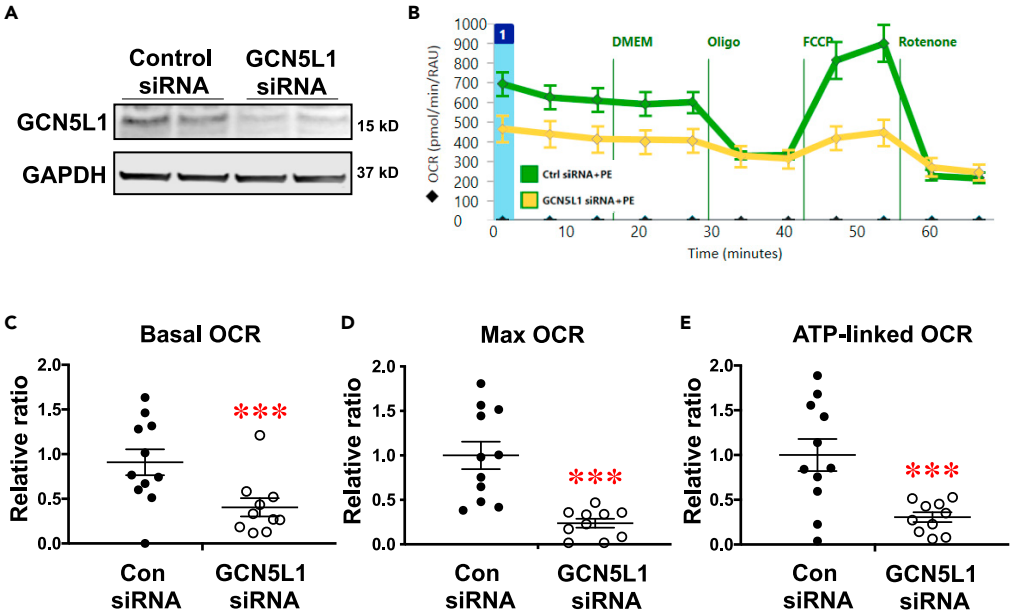

Figure 4. Loss of GCN5L1 expression in cardiomyocytes impairs mitochondrial bioenergetics

(A) Knockdown of GCN5L1 by siRNA.

(B–E) Knockdown of GCN5L1 with siRNA in NRCMs resulted in impaired basal and (C) maximum oxygen consumption rate (OCR), and (D) decreased ATP synthesis-linked OCR, following treatment with phenylephrine (n = 8). Data are shown as means ± SEM. ***p < 0.001.

GCN5L1 adenovirus, and found that TFAM acetylation was significantly upregulated in response to GCN5L1 overexpression (Figure 6D).

Finally, to understand how acetylation of TFAM might impact mtDNA levels in cells, we generated expression plasmids for WT TFAM and for two mutants where four lysine residues (K62/K76/K111/K118) were replaced with glutamine (4KQ) or arginine (4 KR). These four lysine residues of TFAM have previously been reported to be acetylated in proteomic studies,[14] and the substitutions made were designed to model the acetylated (4KQ) and deacetylated (4 KR) state, respectively.[15] Expression of the acetyl-mimetic 4KQ mutant in human cardiac AC16 cells led to a ~20% increase in mtDNA copy number relative to WT TFAM, which trended toward (but did not reach) statistical significance (p = 0.07). Conversely, expression of the deacetylated 4 KR mimetic resulted in a significantly decreased mtDNA copy number relative to the acetylated 4KQ mimetic (Figure 6E), suggesting that acetylation of TFAM is correlated with an increase in mtDNA levels. Combined, these data suggest that GCN5L1 promotes bioenergetic output in stressed cardiomyocytes by maintaining mtDNA levels and mitochondrial respiratory function through the acetylation and activation of TFAM.

DISCUSSION

Lysine acetylation is recognized as a common post-translational modification of mitochondrial metabolic enzymes.[16] In the heart, mitochondrial targets account for nearly 60% of total acetylated proteins and 64% of acetylation sites.[17] The majority of acetylated proteins identified are enzymes involved in fatty acid metabolism, oxidative phosphorylation, or the tricarboxylic acid cycle,[17] suggesting a possible regulatory role in mitochondrial energy metabolism. However, the role of global changes in lysine acetylation in the control of mitochondrial function remains controversial. For example, quantitative proteomic studies have found low acetylation occupancy rates of candidate regulatory lysine residues of metabolic enzymes, raising questions about the physiological impact of this post-translational modification.[18] More recently, a cardiac-focused study reported that global hyperacetylation of cardiac mitochondrial proteins, using a striated muscle-specific sirtuin 3 and carnitine acetyltransferase double knockout (SIRT3/CrAT DKO) mouse, had little negative impact on mitochondrial respiration or cardiac contractile function after TAC.[19] These findings suggested that non-specific global hyperacetylation of mitochondrial proteins is well tolerated

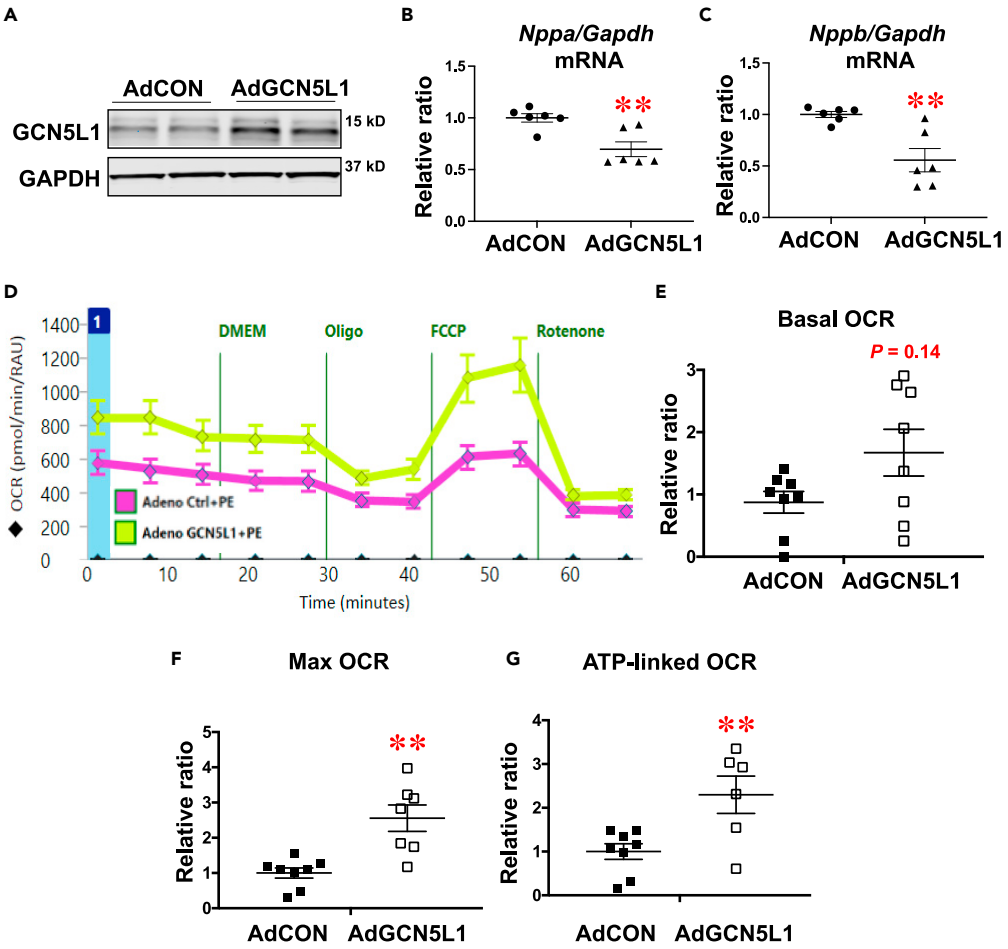

Figure 5. Adenoviral-mediated GCN5L1 overexpression inhibited cardiomyocyte hypertrophy and promoted mitochondrial bioenergetic output

(A–C) Adenoviral overexpression of GCN5L1 attenuated the PE-induced cardiomyocyte hypertrophy, as measured by reduced fetal gene reprograming (n = 6).

(D–G) Adenoviral overexpression of GCN5L1 in NRCMs increased maximal oxygen consumption rate (OCR) and ATP synthesis-linked OCR in the presence of PE (n = 8). Basal respiration was increased with GCN5L1 overexpression but did not reach statistical significance. Data are shown as means ± SEM. *p < 0.05, **p < 0.01, ***p < 0.001.

under certain conditions, thereby questioning the potential physiological relevance of excess lysine acetylation in the hemodynamically stressed heart.

Intriguingly, rather than exacerbating the effects of hemodynamic stress as predicted, global mitochondrial protein hyperacetylation in SIRT3/CrAT DKO mice led to a 15%–20% improvement in survivorship after TAC relative to WT mice over the course of the 16-week study, with a significant improvement being detected in the first three weeks after surgery.[19] These data suggest that rather than being inhibitory as first proposed, increased mitochondrial protein acetylation may promote some level of cardioprotection, particularly in the early stages of hemodynamic stress. Our new data presented here suggest that this may be related to the maintenance of mitochondrial bioenergetics, via GCN5L1-mediated TFAM acetylation, during the early hypertrophic response to pressure overload. In this context, a reduction in mitochondrial protein acetylation (via GCN5L1 downregulation or deletion) would limit mitochondrial bioenergetic output, while hyperacetylation (via SIRT3/CrAT deletion) may in fact be protective by maintaining TFAM acetylation and boosting cardiomyocyte energetics in the early stages of heart failure. Future studies, examining whether cardiac GCN5L1 downregulation remains deleterious in the context of SIRT3 deletion (where TFAM would presumably remain acetylated during TAC), will help to further delineate this pathway.

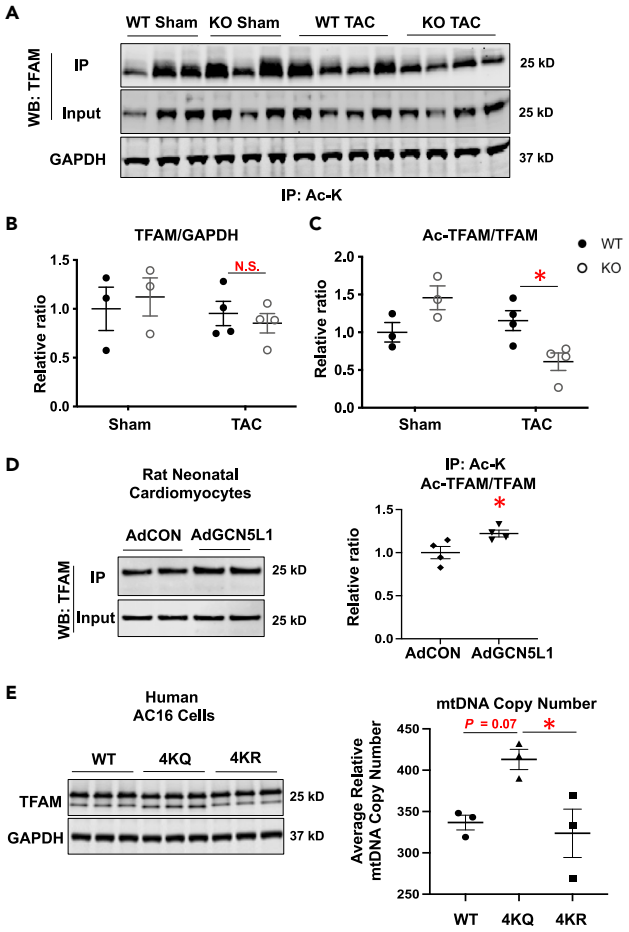

Figure 6. GCN5L1-mediated TFAM acetylation promotes increased mtDNA abundance

(A–C) The acetylation level of TFAM was decreased in cGCN5L1 KO mice subjected to TAC relative to WT controls, without changes in total TFAM protein abundance (n = 3–4).

(D) Adenoviral overexpression of GCN5L1 in NRCMs increased the acetylation of TFAM (n = 4).

(E) Overexpression of acetyl-mimetic 4KQ TFAM in AC16 cells increased total mtDNA copy number relative to the deacetylated-mimetic 4 KR TFAM (n = 3). Data are shown as means ± SEM. *p < 0.05, **p < 0.01, ***p < 0.001.

We previously identified several mitochondrial targets of GCN5L1, including fatty acid oxidation enzymes (long-chain acyl-CoA dehydrogenase, short-chain acyl-CoA dehydrogenase, and hydroxyacyl-CoA dehydrogenase),[11,13] ETC proteins (NDUFA9 from Complex I and ATP5a from ATP synthase),[10] and the glucose oxidation enzyme pyruvate dehydrogenase.[20] Here, we identified a new GCN5L1 target, TFAM, a transcription factor controlling mitochondrial DNA replication and mitochondrial metabolism. We found that the acetylation status of TFAM was reduced in cGCN5L1 KO mice hearts subjected to TAC in comparison with WT controls (Figure 4A). In 293T cells, overexpression of GCN5L1 increased the acetylation level of TFAM, further demonstrating that TFAM is likely a target of GCN5L1-mediated acetylation (Figure 4D). Indeed, the decreased mtDNA level observed in GCN5L1 KO mice hearts after TAC suggests that GCN5L1 potentially regulates mtDNA abundance through the acetylation of TFAM, and *in vitro* modeling of TFAM acetylation supports the hypothesis that hyperacetylation of this protein correlates with higher mtDNA levels (Figure 4E).

Proteomic detection of TFAM acetylation has been reported previously, with an initial characterization in a rat model demonstrating that TFAM was acetylated at a single residue in numerous organs.[21] Several pieces of recent evidence have further suggested that TFAM acetylation is likely to have a regulatory effect on mtDNA gene expression and abundance. Using an acetyl-mimetic model, King et al. (2018) demonstrated that acetylated TFAM is less able to bind to DNA (via a reduced on-rate). This change may limit

the ability of TFAM to maintain DNA compaction and allow fine-tuning of mtDNA-TFAM dynamics,[22] leading to increased mtDNA transcription. Chemical acetylation of TFAM *in vitro* using acetyl-CoA led to several hyperacetylated lysine residues (including the four used in our mutant analyses), which may alter mtDNA topology.[14] Finally, a contemporary study of TFAM post-translational modifications demonstrated that acetylated TFAM increased the processivity of the mitochondrial RNA polymerase POLRMT, allowing this enzyme to more easily move past TFAM roadblocks on mtDNA during transcription.[23]

In the context of the present study, these previous findings would suggest that GCN5L1-mediated acetylation of TFAM allows greater mitochondrial gene transcription and mtDNA abundance, which permits the maintenance of bioenergetic output to meet the demands of hemodynamic stress. We hypothesize that GCN5L1 downregulation in response to pressure overload (as occurs in human or mouse failing hearts; Figures 1A and 1B), or cardiomyocyte-specific deletion of GCN5L1 (Figures 1C–1I), prevents the heart from upregulating bioenergetic output under stress, which aids the progression of cardiac dysfunction. Our findings suggest that mechanisms to maintain GCN5L1 abundance in the stressed heart may represent a potential new therapeutic approach in the treatment of heart failure.

Limitations of the study

We observed that ETC protein levels, mitochondrial complex activity, and mtDNA levels were decreased in cGCN5L1 KO mice in response to TAC. Further work is required to fully determine whether the changes observed were directly due to a loss of GCN5L1 activity on specific target proteins, or were secondary to the general effect of the more advanced heart failure phenotype observed in cGCN5L1 KO mice (relative to WT mice) at the same stage after TAC.

GCN5L1 has multiple mitochondrial targets;[11,13] therefore, other biological pathways may be mediated by GCN5L1 loss in heart failure in addition to its impact on TFAM. To ultimately address these questions in a future study, a rescue experiment using TFAM overexpressed in cGCN5L1 KO mice subject to TAC will be required.

Finally, while this manuscript was in revision, it was reported that GCN5L1 is responsible for the acetylation of TFAM at K76 (one of the lysine residues tested by our *in vitro* studies) in an acute kidney injury model.[24] The authors of this contemporary report suggested that the GCN5L1-TFAM interaction in the kidney occurred in the cytosol, and that GCN5L1-mediated acetylation negatively impacted the import of TFAM into mitochondria.[24] Further work will be required to determine whether this cytosolic interaction is specific to the kidney, and whether the K76 modification—which occurs over 30 amino acids after the end of the N-terminal mitochondrial targeting sequence on TFAM—can indeed regulate the import of endogenous TFAM in multiple tissues.

STAR★METHODS

Detailed methods are provided in the online version of this paper and include the following:

- KEY RESOURCES TABLE
- RESOURCE AVAILABILITY
  - Lead contact
  - Materials availability
  - Data and code availability
- EXPERIMENTAL MODEL AND SUBJECT DETAILS
  - Animals
  - Human subjects
  - Cell lines
  - Primary cell cultures
- METHOD DETAILS
  - TAC procedure
  - Mitochondrial DNA copy number and mitochondrial protein level assessment
  - Mitochondrial isolation and activity assay measurement
  - Cardiac myocytes and cell line studies
  - Mitochondrial bioenergetics measurements in cultured cardiac myocytes
  - Western blot and immunoprecipitation

- Quantitative RT-PCR
- Statistics

SUPPLEMENTAL INFORMATION

Supplemental information can be found online at https://doi.org/10.1016/j.isci.2023.106942.

ACKNOWLEDGMENTS

We thank the University of Pittsburgh Small Animal Ultrasonography Core, and funding for the echocardiography equipment from the NIH Instrumentation Program (NIH 1S10OD023684). The Center for Metabolism and Mitochondrial Medicine was supported by funding from the Pittsburgh Foundation to M.J.J. (MR2020 109502). The work was supported by NHLBI K08 HL157616, a UPMC HVI Fellows Research Award, and a Samuel and Emma Winters Foundation Award to M.Z.; by NHLBI K08 HL130604, American Heart Association Innovative Project Award #18IPA34170219, and R03 HL164393 to N.F.; and by NHLBI K22 HL116728, R01 HL132917, and R01 HL156874 to I.S.

AUTHOR CONTRIBUTIONS

M.Z., N.F., and I.S. designed the experiments. M.Z., N.F., D.T., M.S., J.M., C.M., X.Y., Z. P., K.R., and D.G. obtained the data. M.J.J. and M.N.S. provided critical reagents or expertise. M.Z., N.F., S.S., B.K., M.W.S., and I.S. analyzed the data. M.Z. wrote the manucript, I.S. edited the manuscript and made revisions.

DECLARATION OF INTERESTS

The authors declare no competing interests.

INCLUSION AND DIVERSITY

We support the inclusive, diverse, and equitable conduct of research.

Received: November 18, 2022
Revised: April 11, 2023
Accepted: May 19, 2023
Published: May 23, 2023

REFERENCES

1. Benjamin, E.J., Virani, S.S., Callaway, C.W., Chamberlain, A.M., Chang, A.R., Cheng, S., Chiuve, S.E., Cushman, M., Delling, F.N., Deo, R., et al. (2018). Heart disease and stroke statistics-2018 update: a report from the American heart association. Circulation *137*, e67–e492. https://doi.org/10.1161/CIR.0000000000000558.

2. Yancy, C.W., Jessup, M., Bozkurt, B., Butler, J., Casey, D.E., Jr., Drazner, M.H., Fonarow, G.C., Geraci, S.A., Horwich, T., Januzzi, J.L., et al. (2013). 2013 ACCF/AHA guideline for the management of heart failure: a report of the American college of cardiology foundation/American heart association task force on practice guidelines. J. Am. Coll. Cardiol. *62*, e147–e239. https://doi.org/10.1016/j.jacc.2013.05.019.

3. Yancy, C.W., Jessup, M., Bozkurt, B., Butler, J., Casey, D.E., Jr., Colvin, M.M., Drazner, M.H., Filippatos, G.S., Fonarow, G.C., Givertz, M.M., et al. (2017). 2017 ACC/AHA/HFSA focused update of the 2013 ACCF/AHA guideline for the management of heart failure: a report of the American college of cardiology/American heart association task force on clinical practice guidelines and the heart failure society of America. J. Am. Coll. Cardiol. *70*, 776–803. https://doi.org/10.1016/j.jacc.2017.04.025.

4. Doehner, W., Frenneaux, M., and Anker, S.D. (2014). Metabolic impairment in heart failure: the myocardial and systemic perspective. J. Am. Coll. Cardiol. *64*, 1388–1400. https://doi.org/10.1016/j.jacc.2014.04.083.

5. Bhatt, K.N., and Butler, J. (2018). Myocardial energetics and heart failure: a Review of recent therapeutic trials. Curr. Heart Fail. Rep. *15*, 191–197. https://doi.org/10.1007/s11897-018-0386-8.

6. Bayeva, M., Gheorghiade, M., and Ardehali, H. (2013). Mitochondria as a therapeutic target in heart failure. J. Am. Coll. Cardiol. *61*, 599–610. https://doi.org/10.1016/j.jacc.2012.08.1021.

7. Ventura-Clapier, R., Garnier, A., and Veksler, V. (2008). Transcriptional control of mitochondrial biogenesis: the central role of PGC-1alpha. Cardiovasc. Res. *79*, 208–217. https://doi.org/10.1093/cvr/cvn098.

8. Taherzadeh-Fard, E., Saft, C., Akkad, D.A., Wieczorek, S., Haghikia, A., Chan, A., Epplen, J.T., and Arning, L. (2011). PGC-1alpha downstream transcription factors NRF-1 and TFAM are genetic modifiers of Huntington disease. Mol. Neurodegener. *6*, 32. https://doi.org/10.1186/1750-1326-6-32.

9. Ikeuchi, M., Matsusaka, H., Kang, D., Matsushima, S., Ide, T., Kubota, T., Fujiwara, T., Hamasaki, N., Takeshita, A., Sunagawa, K., and Tsutsui, H. (2005). Overexpression of mitochondrial transcription factor a ameliorates mitochondrial deficiencies and cardiac failure after myocardial infarction. Circulation *112*, 683–690. https://doi.org/10.1161/CIRCULATIONAHA.104.524835.

10. Scott, I., Webster, B.R., Li, J.H., and Sack, M.N. (2012). Identification of a molecular component of the mitochondrial acetyltransferase programme: a novel role for GCN5L1. Biochem. J. *443*, 655–661. https://doi.org/10.1042/BJ20120118.

11. Thapa, D., Zhang, M., Manning, J.R., Guimarães, D.A., Stoner, M.W., O'Doherty, R.M., Shiva, S., and Scott, I. (2017). Acetylation of mitochondrial proteins by GCN5L1 promotes enhanced fatty acid oxidation in the heart. Am. J. Physiol. Heart Circ. Physiol. *313*, H265–H274. https://doi.org/10.1152/ajpheart.00752.

12. Thapa, D., Manning, J.R., Stoner, M.W., Zhang, M., Xie, B., and Scott, I. (2020). Cardiomyocyte-specific deletion of GCN5L1 in mice restricts mitochondrial protein hyperacetylation in response to a high fat diet. Sci. Rep. *10*, 10665. https://doi.org/10.1038/s41598-020-67812-x.

13. Thapa, D., Wu, K., Stoner, M.W., Xie, B., Zhang, M., Manning, J.R., Lu, Z., Li, J.H., Chen, Y., Gucek, M., et al. (2018). The protein acetylase GCN5L1 modulates hepatic fatty acid oxidation activity via acetylation of the mitochondrial beta-oxidation enzyme HADHA. J. Biol. Chem. *293*, 17676–17684. https://doi.org/10.1074/jbc.AC118.005462.

14. Fang, Y., Akimoto, M., Mayanagi, K., Hatano, A., Matsumoto, M., Matsuda, S., Yasukawa, T., and Kang, D. (2020). Chemical acetylation of mitochondrial transcription factor A occurs on specific lysine residues and affects its ability to change global DNA topology. Mitochondrion *53*, 99–108. https://doi.org/10.1016/j.mito.2020.05.003.

15. Gorsky, M.K., Burnouf, S., Dols, J., Mandelkow, E., and Partridge, L. (2016). Acetylation mimic of lysine 280 exacerbates human Tau neurotoxicity in vivo. Sci. Rep. *6*, 22685. https://doi.org/10.1038/srep22685.

16. Lu, Z., Scott, I., Webster, B.R., and Sack, M.N. (2009). The emerging characterization of lysine residue deacetylation on the modulation of mitochondrial function and cardiovascular biology. Circ. Res. *105*, 830–841. https://doi.org/10.1161/CIRCRESAHA.109.204974.

17. Foster, D.B., Liu, T., Rucker, J., O'Meally, R.N., Devine, L.R., Cole, R.N., and O'Rourke, B. (2013). The cardiac acetyl-lysine proteome. PLoS One *8*, e67513. https://doi.org/10.1371/journal.pone.0067513.

18. Baeza, J., Smallegan, M.J., and Denu, J.M. (2016). Mechanisms and dynamics of protein acetylation in mitochondria. Trends Biochem. Sci. *41*, 231–244. https://doi.org/10.1016/j.tibs.2015.12.006.

19. Davidson, M.T., Grimsrud, P.A., Lai, L., Draper, J.A., Fisher-Wellman, K.H., Narowski, T.M., Abraham, D.M., Koves, T.R., Kelly, D.P., and Muoio, D.M. (2020). Extreme acetylation of the cardiac mitochondrial proteome does not promote heart failure. Circ. Res. *127*, 1094–1108. https://doi.org/10.1161/CIRCRESAHA.120.317293.

20. Thapa, D., Zhang, M., Manning, J.R., Guimarães, D.A., Stoner, M.W., Lai, Y.C., Shiva, S., and Scott, I. (2019). Loss of GCN5L1 in cardiac cells limits mitochondrial respiratory capacity under hyperglycemic conditions. Phys. Rep. *7*, e14054. https://doi.org/10.14814/phy2.14054.

21. Dinardo, M.M., Musicco, C., Fracasso, F., Milella, F., Gadaleta, M.N., Gadaleta, G., and Cantatore, P. (2003). Acetylation and level of mitochondrial transcription factor A in several organs of young and old rats. Biochem. Biophys. Res. Commun. *301*, 187–191. https://doi.org/10.1016/s0006-291x(02)03008-5.

22. King, G.A., Hashemi Shabestari, M., Taris, K.K.H., Pandey, A.K., Venkatesh, S., Thilagavathi, J., Singh, K., Krishna Koppisetti, R., Temiakov, D., Roos, W.H., et al. (2018). Acetylation and phosphorylation of human TFAM regulate TFAM-DNA interactions via contrasting mechanisms. Nucleic Acids Res. *46*, 3633–3642. https://doi.org/10.1093/nar/gky204.

23. Reardon, S.D., and Mishanina, T.V. (2022). Phosphorylation and acetylation of mitochondrial transcription factor A promote transcription processivity without compromising initiation or DNA compaction. J. Biol. Chem. *298*, 101815. https://doi.org/10.1016/j.jbc.2022.101815.

24. Lv, T., Zhang, Y., Ji, X., Sun, S., Xu, L., Ma, W., Liu, Y., and Wan, Q. (2022). GCN5L1-mediated TFAM acetylation at K76 participates in mitochondrial biogenesis in acute kidney injury. J. Transl. Med. *20*, 571. https://doi.org/10.1186/s12967-022-03782-0.

25. Manning, J.R., Thapa, D., Zhang, M., Stoner, M.W., Traba, J., McTiernan, C.F., Corey, C., Shiva, S., Sack, M.N., and Scott, I. (2019). Cardiac-specific deletion of GCN5L1 restricts recovery from ischemia-reperfusion injury. J. Mol. Cell. Cardiol. *129*, 69–78. https://doi.org/10.1016/j.yjmcc.2019.02.009.

26. Yang, X., Zhang, M., Xie, B., Peng, Z., Manning, J.R., Zimmerman, R., Wang, Q., Wei, A.C., Khalifa, M., Reynolds, M., et al. (2022). Myocardial brain-derived neurotrophic factor regulates cardiac bioenergetics through the transcription factor Yin Yang 1. Cardiovasc. Res. *119*, 571–586. https://doi.org/10.1093/cvr/cvac096.

27. Jiang, M., Kauppila, T.E.S., Motori, E., Li, X., Atanassov, I., Folz-Donahue, K., Bonekamp, N.A., Albarran-Gutierrez, S., Stewart, J.B., and Larsson, N.G. (2017). Increased total mtDNA copy number cures male infertility despite unaltered mtDNA mutation load. Cell Metabol. *26*, 429–436.e4. https://doi.org/10.1016/j.cmet.2017.07.003.

28. Zhang, M., He, Q., Chen, G., Li, P.A., Ross, M.A., Granger, J.M., Luczak, E.D., Bedja, D., Jiang, H., and Feng, N. (2020). CaMKII exacerbates heart failure progression by activating class I HDACs. Neurodegener. Dis. *20*, 73–83. https://doi.org/10.1016/j.yjmcc.2020.09.007.

29. Wang, L., Liu, Z., Cao, X., Li, J., Zhang, A., Sun, N., Yang, C., and Zhang, K. (2017). GCN5L1 modulates cross-talk between mitochondria and cell signaling to regulate FoxO1 stability and gluconeogenesis. Nat. Commun. *21*, 523–530. https://doi.org/10.1038/s41467-017-00521-8.

STAR★METHODS

KEY RESOURCES TABLE

REAGENT or RESOURCE	SOURCE	IDENTIFIER
Antibodies		
Oxphos	Abcam	Ab110413; RRID: AB_2629281
TFAM	Cell signaling Technologies	#8076S; RRID: AB_10949110
GAPDH	Cell signaling Technologies	#5174; RRID: AB_10622025
α-Tubulin	Cell signaling Technologies	#2148; RRID: AB_2288042
VDAC	Cell signaling Technologies	#4866; RRID: AB_2272627
Acetylated lysine	Cell signaling Technologies	#9441; RRID: AB_331805
GCN5L1	Scott et al. 2012	N/A
Bacterial and virus strains		
Adenovirus control	Wang,et al. 2017	N/A
Adenovirus GCN5L1	Wang,et al. 2017	N/A
Biological samples		
Human heart	University of Pittsburgh	N/A
Chemicals, peptides, and recombinant proteins		
Phenylephrine	Sigma	P2126
Collagenase type II	Worthington	#LS004176
Critical commercial assays		
Qiagen Qproteome Mitochondrial Isolation kit	*Qiagen*	37612
Lipofectamine™ RNAiMAX Transfection Reagent	Thermo Fisher Scientifics	13778150
NovaQUANT Human Mitochondrial to Nuclear DNA Ratio Kit	Sigma	72620-1KIT-M
MitoCheck Complex I activity kit	Cayman Chemical Company	700930
MitoCheck Complex IV activity kit	Cayman Chemical Company	700990
Experimental models: Cell lines		
293T	American Type Culture Collection (ATCC)	#CRL-3216
AC16	EMD Millipore	SCC109
Oligonucleotides		
GCN5L1 siRNA	Origene	#SR15522
Mouse CTGF QuantiTech primers	Qiagen	QT00096131
Rat Ppargc1a QuantiTech primers	Qiagen	QT00189196
Human Gapdh QuantiTech primers	Qiagen	QT00273322
Mouse Gapdh QuantiTech primers	Qiagen	QT01658692
Rat Gapdh QuantiTech primers	Qiagen	QT01082004
Human Bloc1s1 QuantiTech primers	Qiagen	QT00016002
Mouse Bloc1s1 QuantiTech primers	Qiagen	QT01063069
Mouse Sirt3 QuantiTech primers	Qiagen	QT00147280
Rat Bloc1s1 QuantiTech primers	Qiagen	QT01594159
Mouse Nppa Taqman primer/probe	Thermo Fisher Scientifics	Mm01255747_g1
Mouse Nppb Taqman primer/probe	Thermo Fisher Scientifics	Mm01255770_g1
Rat Nppb QuantiTech primers	Thermo Fisher Scientifics	Rn00580641_m1

(*Continued on next page*)

Continued

REAGENT or RESOURCE	SOURCE	IDENTIFIER
Rat Nppa QuantiTech primers	Thermo Fisher Scientifics	Rn00561661_m1
MT-ATP6	Thermo Fisher Scientifics	Mm03649417_g1
MT-ND2	Thermo Fisher Scientifics	Mm04225288_s1
18s RNA	Thermo Fisher Scientifics	HS99999901-s1
Software and algorithms		
Prism 9	GraphPad	http://www.graphpad.com/scientific-software/prism/
Image J	NIH	http://imagej.nih.gov/ij/

RESOURCE AVAILABILITY

Lead contact

Further information, or requests for reagents or resources, should be directed to the lead contact, Dr. Iain Scott (Email: iain.scott@pitt.edu).

Materials availability

All unique/stable reagents generated in this study are available from the lead contact with a completed Materials Transfer Agreement.

Data and code availability

- All data reported in this paper will be shared by the lead contact upon request.
- This paper does not report original code.
- Amu additional information required to reanalyze the data reported in this paper is available from the lead contact upon request.

EXPERIMENTAL MODEL AND SUBJECT DETAILS

Animals

Study procedures were approved by the University of Pittsburgh Animal Care and Use Committees (IACUC) in accordance with National Institutes of Health guidelines. Mice were housed at 22±2°C with lights switched on and off every 12 hours from 7am to 7pm. Mice were provided *ad libitum* access to food and water. Floxed GCN5L1 KO mice were reported previously.[25] Cardiac-specific GCN5L1 KO mice (cGCN5L1 KO mice) were generated by crossing the floxed GCN5L1 mice with αMHC-Cre mice (Jackson Lab, Stock # 011038). Sexes are evenly distributed in the experimental groups. Sample size was 3-15 in each group, and varied by study. Studies were performed with 2-5 months old mice and 1 year old mice. Pregnant Sprague Dawley rats (gestational age 18 days) were purchased from Envigo.

Human subjects

Human heart failure tissues were obtained from transplant recepients with non-ischemic cardiomyopathy at the University of Pittsburgh Medical Center with Institutional Review Board (IRB) approval and informed consents. The control human heart tissues were kindly donated by Dr. Johnathan Kirk, and were obtained via study protocols approved by the IRB at Loyola University Chicago. All samples were preserved in cold cardioplegic solution and transported to the laboratory. Heart tissue was then snap frozen in liquid nitrogen and then stored at -80°C until assay. The Immune status, previous procedure and drug test data are unknown. Control group – N = 5, Mean Age = 60.4 +/- 7.4 (S.D.), 4M/1F, 3 white non-Hispanic, 1 white Hispanic, 1 African American/Black. Non-ischemic failing group – N = 10, Mean Age = 46.1 +/- 16.1 (S.D.), 6M/4F, 8 white non-Hispanic, 2 African American/Black. No significant difference in age between groups (Two-tailed t-test, $P = 0.10$). Full details of the cohorts used are available in Table S1.

Cell lines

293T cells were purchased from ATCC and AC16 cells were purchased from EMD Millipore. Cells were cultures in DMEM (with high glucose and pyruvate, Thermal Fisher Cat # 11995073) with 10% fetal bovine serum (FBS). Cells were cultured at 37±0.5°C with 5% CO_2.

Primary cell cultures

Neonatal Sprague Dawley rat myocytes were isolated from 1-3 days old neonate hearts, and the sex of neonates was not observable at that time point. All cells from the neonatal hearts were pooled for experiments. Cells were cultured in DMEM (with high glucose and pyruvate, Invitrogen Cat # 11995073) with 10% FBS for the first day, and then FBS was replaced by insulin-Transferrin-Selenium (ITS, Thermal Fisher Cat # 41400045) the next day. Cells were cultured at 37 $\pm$0.5°C with 5% CO_2.

METHOD DETAILS

TAC procedure

TAC procedure was performed as previously described.[26] Briefly, sterile surgery was performed in our dedicated facility. Anesthesia was induced with 3.0% isoflurane, and maintained by ventilator at 2.0% isoflurane. Skin was shaved and steriled with povidone-iodine. An incision was made to the immediate left of the sternum, the 2nd and 3rd ribs were cut, and blunt isolation was done to expose the aortric arch. A 7-0 proline suture tie was placed around the aortic arch between the bronchiocephalic artery and left common carotid artery, and tightened around a 27- or 26-gauge needle. Once the tie was fixed, the needle was removed, and the suture/stenosis remained. The chest was then closed with a 6-0 proline suture and 5-0 silk suture. Serial echocardiography was performed in sedated mice (TAC) and conscious mice (12-months-old) as described previously.[26]

Mitochondrial DNA copy number and mitochondrial protein level assessment

Mitochondrial DNA and genomic DNA were isolated from mouse hearts using QIAamp Fast DNA Tissue Kit (Qiagen #51404) according to the manufacturer's instructions. mtDNA copy number was assessed with Mitochondrially Encoded NADH:Ubiquinone Oxidoreductase Core Subunit 2, (mt-ND2), or Mitochondrially Encoded ATP Synthase Membrane Subunit 6, (mt-ATP6)/genomic DNA (18s RNA) ratio as previously described.[27] The Taqman primers were obtained from Thermo Fisher Scientific (MT-ATP6: Mm03649417_g1, MT-ND2: Mm04225288_s1, 18 sRNA gene: Hs99999901_s1). Total mitochondrial DNA copy number was analyzed using the NovaQUANT Human Mitochondrial to Nuclear DNA Ratio Kit (Sigma #72620-1KIT-M). Mitochondrial proteins level was evaluated by Western Blot using OXPHOS cocktail antibodies (Abcam, #ab110413). Mitochondrial proteins were isolated using the Qiagen QProteome Mitochondrial Isolation kit according to the manufacturer's instruction.[20]

Mitochondrial isolation and activity assay measurement

Mitochondria were isolated from heart tissue using the Qiagen QProteome Mitochondrial Isolation kit. Isolated mitochondrial pellets were lysed in RIPA buffer for western blot preparation. Alternatively, mitochondria were subject to freeze-thaw 8 times in RIPA buffer, and 5 μg of lysate was used for mitochondrial Complex I or IV activity measurements using Cayman MitoCheck Complex I & IV activity kits.

Cardiac myocytes and cell line studies

Adult myocytes were isolated using Langendorff perfusion setup as previously described.[26] Adult mice were anethetized with isoflurane, sacrificed by cervical dislocation, and hearts immediately harvested and washed in Tyrode's solution (130 mM NaCl, 5.4 mM KCl, 1 mM MgCl2, 0.6 mM Na2HPO4, 10 mM glucose and 10 mM HEPES, pH 7.4 oxygenated with 95% O_2/5% CO_2 [v/v]). The hearts were then cannulated via the ascending aorta, and purfused with circulated and oxygenated Tyrode's solution at 37°C until the perfusate ran clear. Perfusion buffer was then changed to Tyrode's solution containing collagenase II and protease type XIV for ~10 min. Well-digested hearts were subsequently removed from the cannula and isolated ventricles cut into small pieces, followed by pipetting to aid tissue disruption, and mesh filtering. Myocyte viability was confirmed by microscope as rod-shaped cells. Isolated myocytes were left upright in the tube for 10 min, with live myocytes being enriched as they settled to the bottom of the tube by gravity. Neonatal rat cardiomyocytes (NRCMs) were freshly isolated as described previously.[28] Briefly, hearts were quickly removed from one to three day-old Sprague Dawley neonates, and cardiac myocyte isolation was achieved by digestion with 0.04% trypsin and type II collagenase (0.4mg/ml; Worthington #LS004176) in Krebs-Henseleit bicarbonate buffer at 37°C. Non-cardiomyocyte cells were removed by rapid attachment (90 minutes incubation in culture dishes). Cardiomyocytes were plated at the density of 2x10^5/ml in DMEM containing 10% FBS and 0.1 mM BrdU to prevent the growth of fibroblasts. Twenty-four hours after cells plating, the medium was changed to serum-free DMEM containing 0.1% insulin-transferrin-selenium (Thermo Fisher Scientific #41400045). 293T cells were obtained from ATCC (#CRL-3216), and cultured in

DMEM containing 10% FBS. AC16 cells were obtained from EMD Millipore (#SCC109) and maintained in DMEM containing 10% FBS.

Mitochondrial bioenergetics measurements in cultured cardiac myocytes

Oxygen consumption rate (OCR) was measured in NRCMs transfected with control siRNA, GCN5L1 siRNA, control adenovirus, or GCN5L1 adenovirus using the Seahorse XF system (Seahorse Bioscience) as described previously.[20] Basal OCR in each well was measured, followed by serial treatment with FCCP (7.5 μmol/L) and rotenone (2 μmol/L). Each experiment was repeated to ensure reproducibility, and the data presented are technical replicates (N = 8-11) of a single representative study. NRCMs were transfected with GCN5L1 siRNA (Origene # SR15522) and control siRNA using Lipofectamine™ RNAiMAX Transfection Reagent (Thermo Fisher Scientific #13778150) according to the manufacturer's protocol. The adenovirus overexpressing GCN5L1 was previously reported.[29] Briefly, adenoviruses were produced using the Adeasy Adenoviral system (Agilent), and a multiplicity of infection (MOI) of 10 was used for all the experiments. NRCMs were treated with phenylephrine (20 μM; Sigma #P6126), 24 hours after siRNA transfection, for 48 hours before use or harvest. The human TFAM WT, 4KQ (K62Q/K76Q/K111Q/K118Q), and 4KR (K62R/K76R/K111R/K118R) plasmids were custom synthesized by Genscript, and transiently transfected for 48 hours into AC16 cells using Lipofectamine as above.

Western blot and immunoprecipitation

Protein extracts were prepared in RIPA lysis buffer (Thermo Fisher Scientific #89900) from snap-frozen heart tissues. Protein concentration was measured by BCA assay (Thermo Fisher Scientific #23227). Immunoprecipitation of tissue/cell lysates was performed in RIPA buffer, with equal amounts of protein used for immunoprecipitation assay with rabbit acetyl-lysine (Ac-K) antibody (Cell Signaling Technology #9441) and protein G agarose beads (Cell Signaling Technology #37478) overnight at 4°C. Beads were washed 4 times with RIPA buffer, and then eluted directly with LDS sample buffer (Thermo Fisher Scientific #B0007) at 95°C for 5 mins. Protein electrophoresis was performed on 4–12% Bis-Tris NuPage gels (Thermo Fisher Scientific #NW04120BOX). The Bio-Rad Trans-Blot Turbo Transfer System was used for protein transfer to nitrocellulose membranes. The related secondary antibodies used were from LI-COR Biosciences, and blots were quantified using Image J software (NIH). GCN5L1 antibody was used as previously reported.[10] Oxphos Cocktail antibody (#ab110413) was from Abcam. The TFAM (#8076S), α-tubulin (#2148), GAPDH (#5174), and VDAC (#4866) antibodies were from Cell Signaling Technologies.

Quantitative RT-PCR

Total RNA was extracted from NRCMs or snap-frozen heart tissues using TRIzol reagent (Thermo Fisher Scientific). Reverse transcription was conducted using the High-Capacity cDNA Reverse Transcription Kit (Thermo Fisher Scientific). Taqman primers (Thermo Fisher Scientific) were used for quantitative RT-PCR analysis: mouse PPARGC1A (Mm01208835_m1), and mouse TFAM (Mm00447485_m1).

Statistics

Data were compared within groups using one-way or two-way ANOVA with Tukey's Post Hoc Test using GraphPad Prism version 9.0. Unpaired student's *t*-test was used for comparison between two groups. All tests were two-tailed and a *P* value of less than 0.05 was considered significant. All values are represented as the mean ± SEM.